Preparation and photocatalytic performance of ZnO nanorods on zinc foil

JI-GUO HUANG[a], JI-CHUN SHI[a], GANG LIU[a], XIAO-DI HU[a], LI-LI DONG[b,c,*], XIAO-GUANG ZHAO[a], XING-JUAN LIU[a]

[a]*Key Laboratory of Groundwater Resources and Environment, Ministry of Education, Jilin University, Changchun 130026, PR China*

[b]*Key Laboratory of Songliao Aquatic Environment, Ministry of Education, Jilin Jianzhu University, Changchun 130118, PR China*

[c]*School of Environment, Northeast Normal University, Changchun 130117, PR China*

ZnO nanorods were prepared by the solution-phase approach and the hydrothermal method directly on zinc foils at low reaction temperature. The composition, morphology of ZnO nanorod structures were characterized by X-ray diffraction (XRD) and scanning electron microscope (SEM). The results confirmed that the uniformly sized and highly vertically aligned ZnO nanorod arrays prepared by the solution-phase approach exhibited better photocatalytic activity in the degradation of methylene blue under visible light. While the hydrothermal method only prepared clusters of ZnO nanorod arrays which oriented all kinds of directions and possessed uneven diameters and worse photocatalytic activity. Furthermore, the concentration, temperature and time-dependent experiments to prepare ZnO nanorods were conducted. It could be concluded that the optimum preparing conditions were 0.05 mol/L mixture, 70℃ and 48h, respectively. Moreover, the large-sized ZnO nanorod arrays photocatalysts which possessed relatively good reusable and stable capability could be easily separated. ZnO nanorod arrays prepared by the solution-phase approach were promising photocatalysts which could be potentially applied for pollution disposal with low-cost.

(Received February 27, 2014; accepted July 10, 2014)

Keywords: ZnO nanorods, Zinc foils, Photocatalytic, Methylene blue

1. Introduction

ZnO has been recognized as one of the most promising II–VI compound semiconductor with a wide band gap (3.37 eV). It has been extensively studied because of its functional applications in gas sensors [1,2] electronic and optoelectronic devices [3], solar cells [4], field-emission devices [5] and photocatalysts [6,7]. The environmental protection applications of ZnO photocatalytic activity are related to air purification [9], water purification [10], and hazardous waste remediation [11]. Currently, gas-phase and solution-phase syntheses are the two main methods to fabricate ZnO nanostructures. To optimize the photocatalytic performances of ZnO nanostructures, researchers have also focused many efforts on developing the method of preparing ZnO nanostructures [12]. In addition, various morphologies such as nanowires [4,13], nanoneedles [14], nanotube [15], nanobelts [16,17], nanoflowers [18,19], nanorods [20,21] structures have been prepared.

Recently, many reports devote to researching the effectiveness of nanostructured ZnO powder in degrading organic pollutants [22-24]. However, it is difficult to separate the conventional ZnO powder photocatalyst from the reacting aqueous suspension which is a major problem for application in water treatment [25]. To overcome this disadvantage, the ZnO nanorod structures, especially well-aligned ZnO nanorod structures with high stability and convenient reuse could be prepared, which will extend the industrial applications of ZnO nanorod structures in environmental treatment.

Currently, photocatalysts are usually used to degrade pollutants under UV light. If photocatalysts that could decompose pollutants under visible light or sunlight could be prepared, it would greatly reduce the operating costs of photocatalysis [26].

Several synthetic approaches have been developed, such as chemical vapor deposition [27,28], electro deposition [29,30], hydrothermal [31-33] and solution-phase [34-37]. Although we could produce high-quality ZnO nanostructures by the methods of chemical vapor deposition, electro-deposition, they are high-energy-consumption route. Alternatively, hydrothermal and solution-phase are rather facile, cost-effective, and scale-up methods. In addition, pieces of friable glass, expensive Si wafers or Al_2O_3 are used as substrates, which are small sized and difficult to industrialize. It may be excellent to find a cheap and large substrate to prepare ZnO nanorod structures which could be practically used into engineering application for

wastewater treatment.

In this work, we respectively used the solution-phase approach and the hydrothermal method to prepare ZnO nanorods on a large area of zinc foil in aqueous solution. These two methods were both simple and low-cost, which had no need to precast ZnO nanoparticles as a seed layer onto the substrates. The morphologies of as prepared samples were characterized and their photocatalytic activities were investigated through degradation experiments of methylene blue (MB) under visible light. Moreover, we chose the better method to study further. By adjusting the reaction concentration, time and temperature, the ZnO nanorods which had the best photocatalytic activity could be obtained. Their photocatalytic stabilities were investigated in detail later. This study provided some useful information for the development of a simple, cheap and well immobilized method to prepare relatively good reusable and stable ZnO nanorods, which had good effects on the degradation of MB under visible light.

2. Experimental

2.1 Materials

Zinc foil (99.9% chemical pure) was purchased from Shanghai Sinopharm Chemical Reagent Co., Ltd. Absolute ethanol, formamide, hexamethylenetetramine, Zinc nitrate hexahydrate and methylene blue were respectively obtained commercially from Beijing Chemical Works, Xilong Chemical Co., Ltd, Tianjin Guangfu Science and Technology Development Co., Ltd, Tianjin Guangfu Science and Technology Development Co., Ltd and Research Institute of Guangfu Fine Chemical Engineering in Tianjin. Distilled water was utilized to prepare all aqueous solution and to rinse the photocatalyst samples. All chemicals were of analytical grade, and used without further purification.

2.2. Preparation of ZnO nanorods

A large size of zinc foil (40 mm×75 mm×0.25 mm) was pretreated by ultrasonication (KQ-300DE, 150W) in distilled water and absolute ethanol respectively for 10min, and then dried in air.

Sample A was prepared by the solution-phase approach. Place the pretreated zinc foil vertically into a beaker containing a mixture which ultrasonically mixed 0.05mol/L hexamethylenetetramine (HMT) with equal volume and concentration of zinc nitrate $(ZnNO_3)_2$ aqueous solution, and then cover the beaker with plastic wrap. The reaction system was then maintained at a constant temperature of 70℃ for 24h in a heating oven. Then, the Zinc foil was ultrasonically rinsed in distilled water and absolute ethanol respectively, and finally dried in air.

Sample B was prepared by the hydrothermal method. Place the pretreated zinc foil into a volume of 100 mL polytetrafluoretyhylene (PTFE) cored stainless steel reaction kettle and then add in 5% formamide aqueous solution (v/v). Ditto went for the rest of the operation as Sample A.

2.3. Characterization

The morphologies and crystallographic structures of the samples were imaged by scanning electron microscopy (SEM, HITACHI-SU8000). X-ray diffraction (XRD) patterns were recorded on a PANalytical B.V.-Empyrean diffractometer with Cu Kα radiation (λ=0.154 nm). All of the measurements were carried out at room temperature (25±2 ℃).

2.4. Photocatalytic activities measurement

The photocatalytic degradation of methylene blue (MB) under visible light using as-prepared ZnO nanorods was evaluated at room temperature. The visible light reaction system consisted of a 500 W xenon lamp and a filter [1 mol/L $NaNO_2$ solution in an enclosed vessel (λ> 420 nm)].

A piece of as-prepared ZnO photocatalyst of suspended in a quartz reactor containing 200 mL of 20 mg/L MB aqueous solution with stirring strongly. The reactor was placed at the light intensity (tested by a digital luminance meter, TES-1332A, TES Electrical Electronic Corp) was 8500Lux and the measurements were carried out at room temperature (25±2 ℃). Before lighting, the reaction solution was magnetically stirred in dark for 30 min to ensure adsorption equilibrium of MB. During the experiment process, the concentration of MB aqueous solution was tested on a spectrophotometer (Unico-4802H) at 664nm per hour.

In order to accurately evaluate the recycling and recovery of the photocatalyst, the photocatalytic degradation procedure was performed 3 times. After each time, the used ZnO nanorod photocatalyst was ultrasonically washed with absolute ethanol and distilled water respectively for 10 min to remove the residual MB. The ZnO nanorod photocatalyst was then immersed into a fresh MB solution with the same concentration for another run of the photocatalytic degradation experiment.

3. Results and discussion

3.1. Comparison of ZnO nanorod photocatalysts prepared by the solution-phase approach and the hydrothermal method

The morphologies of the nanorods prepared by the solution-phase approach and the hydrothermal method were shown in Fig. 1a, b. It could be seen that highly oriented arrays consisting of dense hexagonal ZnO nanorods with diameters of 50 ~ 100nm were aligned on the Zn foil surface (Fig. 1a). Cross sectional SEM

observation of the ZnO nanorod arrays from sample A (Fig. 1b) revealed that nanorods with typical lengths of about 1 μm were densely aligned but separated from each other. Their highly preferential growth occurred along the c-axis orientation which was perpendicular to the zinc foil. In the case of the nanorod structures prepared by the hydrothermal method, dense ZnO nanorods could also be observed (Fig. 1c), but their diameters ranged from 50nm to 300nm, which differed from the literature [25]. Moreover, some nanorods densely aligned to be clusters of arrays which oriented all kinds of directions. These results indicated that both of the solution-phase approach and the hydrothermal method could be used to prepare ZnO nanorod arrays on the zinc foils, but with the different diameters and orientations. In addition, the solution-phase approach could be used to prepare uniformly sized and highly vertically aligned nanorod arrays. It was a simple and cheap way to prepare large area and well immobilized ZnO nanorod arrays.

The crystallographic structures of the samples were characterized by XRD measurements. For the two typical samples (Fig. 1d), their diffraction peaks could be well indexed to the hexagonal wurtzite-type ZnO with the lattice constants of a=0.3249nm and c=0.5206nm (JCPDS card No.36-1451), respectively. The XRD patterns of zinc in accordance with the values in the JCPDS card (No. 04-0831) could be perfectly indexed to the hexagonal zinc due to the zinc substrate. Additionally, zinc peaks were substantially weakened which indicated that the crystalline ZnO were grown densely [38]. While the diffraction zinc peaks from sample B were stronger than those from sample A, it revealed that the ZnO nanorod arrays prepared by the solution-phase approach were more densely than those prepared by the hydrothermal method. Specifically, the sharp and intense ZnO peaks (002) confirmed that the as-prepared ZnO structures here were preferentially well oriented in the c-axis directions. Nevertheless, the peaks intensity of sample A was stronger than sample B. It meant that sample A had better crystal quality.

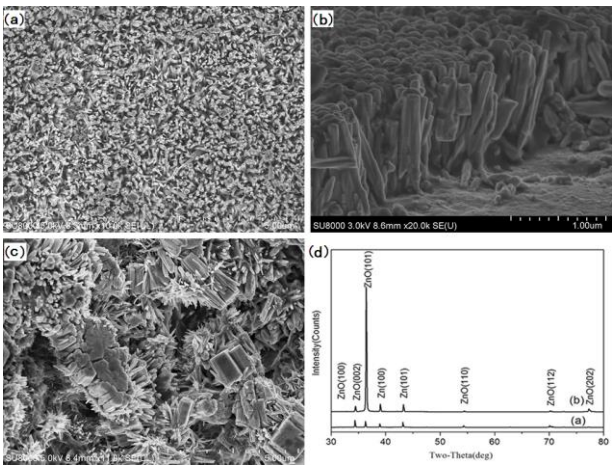

Fig. 1. a SEM image of sample A, b Typical cross-sectional image of sample A, c SEM image of sample B, d XRD patterns of sample A (curve a) and sample B (curve b).

The concentration changes of MB in the presence of different photocatalysts were shown in Fig. 2. Therein, the C_0 represents the remaining concentration of MB after the adsorption equilibrium before lighting, while C represents the remaining concentration of MB lighting for a specific time.

As shown in Fig. 2, after 5h of irradiation, the MB was degraded about 60% under visible irradiation with photocatalyst prepared by the hydrothermal method. While the photocatalyst prepared by the solution-phase approach showed a better photocatalytic activity, about 81% of the MB was degraded, which may be caused by a higher surface area than the latter one due to its smaller and uniform diameters and highly vertical orientation possess. Sample A without irradiation could only decompose 18% of the MB, we could know that the depigmentation of MB was degradation but not adsorption. It could be concluded that ZnO nanorods prepared by the solution-phase approach process better photocatalytic activity than those prepared by the hydrothermal method. Attributed to the unique surface features, the ZnO nanorod arrays had enhanced photocatalytic activity. The excess appearance of the polar ZnO (001) faces in the ZnO nanorod arrays were the most active sites for photocatalytic degradation to organic pollutants, which also led to the significant enhancement of the photocatalytic activity. Our inexpensive ZnO nanorod arrays could prompt the potential application to pollution disposal.

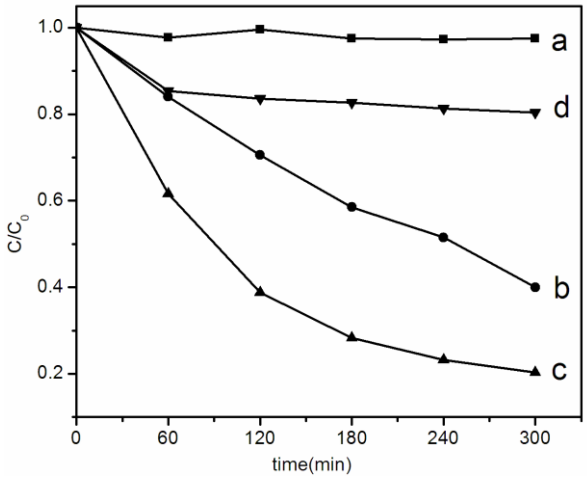

Fig. 2. The photocatalytic degradation of MB [xenon lamp with filter 8500 Lux(＞420nm)] a without photocatalyst, b with sample B, c with sample A, d sample A without irradiation.

3.2. Further study of ZnO nanorod arrays photocatalysts prepared by solution-phase approach

In order to obtain the optimal preparation conditions and investigate the influence factors, we synthesized ZnO nanorod arrays photocatalysts by the solution-phase approach in different conditions and analyzed their

morphologies. These photocatalysts were denoted as T ^{o}C-x M-t h (T, x, t were respectively reaction temperature, concentration and time).

At first, concentration-dependent experiments were carried out at 70 ^{o}C for 24 h. The mixtures were mixed HTM with $ZnNO_3$ aqueous solution by equal volume and the same concentration. Aligned ZnO nanorod arrays could be detected when using 0.0125mol/L mixed aqueous solution, with the diameters ranging from 50nm to 200nm. When the concentration reached to 0.05 mol/L (Fig. 3b), the diameters of ZnO nanorods became more uniform, about 50~100nm. With the increase of concentrations to 0.20 mol/L, the nanorod arrays almost could not be seen from Fig. 3C, because excess of HMT and $Zn(NO_3)_2$ aqueous solution could restrain the vertical growth of ZnO nanorod arrays. In addition, some particles were observed, which suggesting that excessively released OH^- could seriously etch the as-formed ZnO structures [39]. Seen from Fig. 3d, the degradation results also demonstrated that 0.05mol/L could be the best reaction concentration of HMT and $Zn(NO_3)_2$ for the preparation of ZnO nanorod arrays.

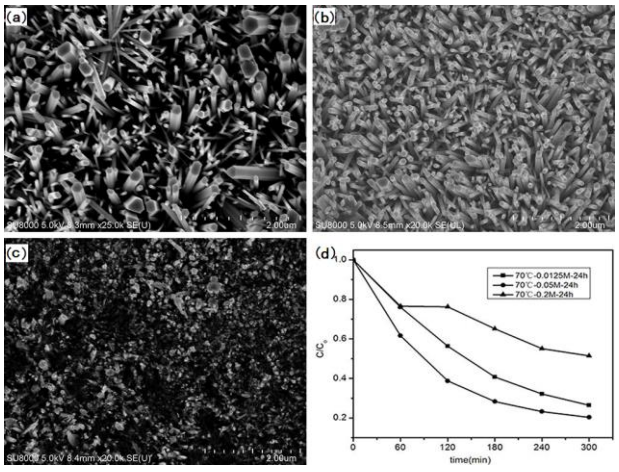

Fig. 3. SEM images of the ZnO nanorod arrays prepared by the solution-phase approach in different concentrations of HMT and $Zn(NO_3)_2$ aqueous solution: a 0.0125mol/L, b 0.05mol/L, c 0.20mol/L, d Degradation of MB [xenon lamp with filter 8500 Lux(＞420nm)] using as-prepared samples.

In this study, the effects of reaction temperature were also considered, as shown in Fig. 4. At 60 ^{o}C, highly vertically aligned ZnO nanorod arrays were formed, with the diameters about 50nm roughly except few of 200nm. At 70 ^{o}C, the diameters of ZnO nanorods varied from 50nm to 100nm, seen from Fig. 4B. Further increasing the temperature to 80 ^{o}C, some ZnO nanorods diameters of about 200nm occurred and started to horizontally grow upon the arrays. The above results revealed that higher temperature could make the ZnO nanorods be cruder and grow horizontally. Fig. 4d showed that 70℃ should be the best reaction temperature for preparing the ZnO nanorod arrays for a relatively high degradation rate of about 80%.

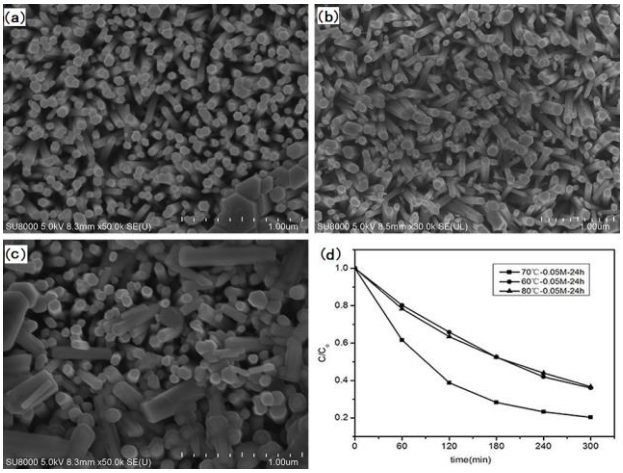

Fig. 4. SEM images of ZnO nanorod arrays prepared in 0.05mol/L HMT and Zn $(NO_3)_2$ aqueous solution at different temperatures for 24 h: a 60 ℃, b 70 ℃, c 80 ℃, d Degradation of MB [xenon lamp with filter 8500 Lux(＞420nm)] using 60 ℃-0.05M-24h, 70 ℃-0.05M-24h and 80 ℃-0.05M-24h.

Further exploring the morphologic evolution of the ZnO nanorod arrays, time-dependent experiments were also performed. The results were shown in Fig. 5. In general, longer reaction time would facilitate the formation of highly crystallized ZnO nanorod arrays [21]. The saturation degree of the $Zn(OH)_4^{2-}$ units was kept at high level with enough reaction time. As expected, the diameters of ZnO nanorods ranged from 50nm to 100nm for 24 h. When the reaction time was increased to 48 h, more $Zn(OH)_4^{2-}$ units were adsorbed onto the surface of ZnO nuclei, which enhance the uniform growth of ZnO nanorods with the diameters to be approximately 100nm. When the reaction time was further extended to 72 h in this study, excessive reaction time facilitated the formation of coarser ZnO nanorod arrays on the zinc foils, with the arrays to be denser and the diameters changed to be about 200nm. At the reaction condition of 70 ^{o}C and 0.05mol/L HMT and Zn $(NO_3)_2$ aqueous solutions, when the zinc foil heated for 48h, the degradation efficiency was up to almost 82%, while 72h to be 73%. The result indicated that longer reaction time made the nanorods thicker, and decreased the effective surface area, which prevented the MB molecules entering into the nanorods.

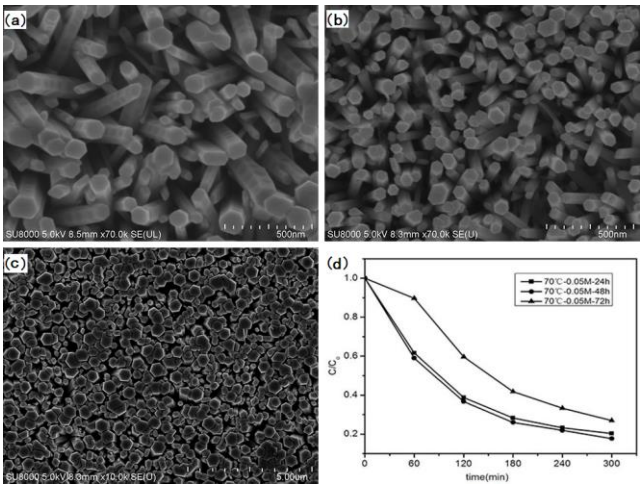

Fig. 5. SEM images of the ZnO nanorod arrays prepared by the solution-phase approach in 0.05mol/L HMT and Zn $(NO_3)_2$ aqueous solutions respectively at 70 ℃ for different reaction time: a 24h, b 48h, c 72h, d Degradation of MB [xenon lamp with filter 8500 Lux(＞420nm)] using 70 ℃-0.05M-24h, 70 ℃-0.05M-48h and 70 ℃-0.05M-72h.

Combined with the SEM images (Fig. 3,4 and 5), the ZnO nanorod arrays composed of more uniform and thinner nanorods showed better photocatalytic performance for MB aqueous solution. We chose 70 ^{o}C-0.05M-48h to measure its light absorption property and do recycle experiment, since it showed the best photocatalytic activity to degrade MB. The ZnO nanorod arrays photocatalysts of 70 ^{o}C-0.05M-48h exhibited remarkable photocatalytic stability after three photocatalytic experiments runs (Fig. 6a). As shown in Fig. 6b, the ZnO nanorod arrays could not be observed after three cycles and they cluster together, which could be the reason of the worse photocatalytic activity.

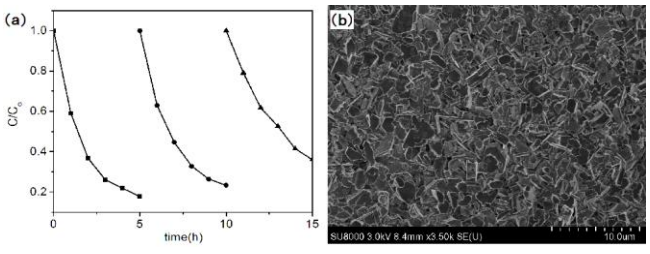

Fig. 6. a Photoactivity stability test [xenon lamp with filter 8500 Lux(＞420nm)] of the photocatalyst of 70 ℃ -0.05M-48h, b SEM image of the photocatalyst of 70 ℃ -0.05M-48h using for 3 times.

4. Conclusion

In summary, we prepared ZnO nanorods on cheap zinc foils at low reaction temperature by the solution-phase approach and the hydrothermal method respectively. For degradation experiments of MB under visible irradiation, the ZnO nanorod arrays prepared by the solution-phase approach showed a better performance due to the more uniform and thinner nanorods. In addition, the optimize preparation condition of the ZnO nanorod arrays photocatalyst was 70℃, 0.05mol/L HMT and Zn $(NO_3)_2$ aqueous solutions and 48h. Furthermore, the large-sized ZnO nanorod arrays photocatalysts possessed relatively good reusability and stability and could be easily separated. Above all, ZnO nanorods prepared by the solution-phase approach were promising photocatalysts which could be potentially applied for pollution disposal with low-cost.

Acknowledgment

Supported by the Science and Technology Foundation of Science and Technology Bureau of Changchun City and the National Natural Science Foundation of China (No.51308252).

References

[1] J. A. Rodriguez, T. Jirsak, J. Dvorak, S. Sambasivan, D. Fischer. J. Phys. Chem. B **104**, 2 (2000).
[2] H. Zhang, R. Wu, Z. Chen, G. Liu, Z. Zhang, Z. Jiao. Cryst. Eng. Comm. **14**, 5 (2012).
[3] Y. Zhao, X. X. Zhang, X. G. Zhao, L. J. Geng. Optoelectron. Adv. Mater.-Rapid Comm. **7**, 1-2 (2013).
[4] M. Law, L. E. Greene, J. C. Johnson, R. Saykally, P. Yang. Natu. Mater. **4**, 6 (2005).
[5] C. H. Liu, J. A. Zapien, Y. Yao, X. M. Meng, C. S. Lee, S. S. Fan, Y. Lifshitz, S. T. Lee. Adv. Mater. **15**, 10 (2003).
[6] C. Hariharan. Appl. Catal. A: Gener. 304, (2006).
[7] A.-J. Wang, Q.-C. Liao, J.-J. Feng, P.-P. Zhang, A.-Q. Li, J.-J. Wang. Cryst. Eng. Comm. **14**, 1 (2012).
[8] Y. Zheng, F. Duan, J. Wu, L. Liu, M. Chen, Y. Xie. J. Molecu. Catal. A: Chem. **303**, 1-2 (2009).
[9] M. R. Hoffmann, S. T. Martin, W. Choi, D. W. Bahnemannt. Chem. Rev. **95**, 1 (1995).
[10] H. Yu, J. Yu, S. Liu, S. Mann. Chem. Mater. **19**, 17 (2007).
[11] J. G. Yu, Y. R. Su, B. Cheng. Adv. Funct. Mater. **17**, 12 (2007).
[12] L. Wang, Y. Zheng, X. Li, W. Dong, W. Tang, B. Chen, C. Li, X. Li, T. Zhang, W. Xu. Thi. Solid. Fil. **519**, 16 (2011).
[13] P. Jiang, J. J. Zhou, H. F. Fang, C. Y. Wang, Z. L. Wang, S. S. Xie. Advan. Funct. Mater. **17**, 8 (2007).
[14] X. Wu, H. Bai, C. Li, G. Lu, G. Shi. Chem. Communica. 15 (2006).
[15] L. Vayssieres, K. Keis, A. Hagfeldt, S.-E. Lindquist. Chem. Mater. **13**, 12 (2001).

[16] X. Wang, Y. Ding, C. J. Summers, Z. L. Wang. J. Phys. Chem. B **108**, 26 (2004).
[17] C.-L. Kuo, T.-J. Kuo, M. H. Huang. J. Phys. Chem. B **109**, 43 (2005).
[18] Y. Feng, M. Zhang, M. Guo, X. Wang. Cryst. Grow. & Des. **10**, 4 (2010).
[19] S. Ashoka, G. Nagaraju, C. N. Tharamani, G. T. Chandrappa. Mater. Lett. **63**, 11 (2009).
[20] J. H. Choy, E. S. Jang, J. H. Won, J. H. Chung, D. J. Jang, Y. W. Kim. Adv. Mater. **15**, 12 (2003).
[21] J.-J. Feng, Z.-Z. Wang, Y.-F. Li, J.-R. Chen and A.-J. Wang. J. Nanopart. Res. 15, 4 (2013).
[22] J. Nishio, M. Tokumura, H. T. Znad, Y. Kawase. J. Hazard. Mater. **138**, 1 (2006).
[23] C.-C. Chen. J. Molecu. Catal. A: Chem. **264**, 1-2 (2007).
[24] K. M. Parida, S. S. Dash, D. P. Das. J. Collo. Interfa. Sci. **298**, 2 (2006).
[25] W. Yuxin, L. Xinyong, L. Guang, Q. Xie, C. Guohua. J. Phys. Chem. B **112**, 19 (2008).
[26] Z. Qianqian, B. Tang, H. Guoxin. J. Hazard. Mater. 198, (2011).
[27] L. L, L. H. B, L. J. C, H. H, W. D. F, F. D. J, L. C, Z. W. F. J. Phys. Chem. B **111**, 5 (2007).
[28] E. Galoppini, J. Rochford. J. Phys. Chem. B **110**, 33 (2005).
[29] B. Marí, M. Mollar, A. Mechkour, B. Hartiti, M. Perales, J. Cembrero. Microelectron. J. **35**, 1 (2004).
[30] X. LF, G. Y, L. Q, Z. JP, X. DS. J. Phys. Chem. B **109**, 28 (2005).
[31] Y. Liu, Z. H. Kang, Z. H. Chen, I. Shafiq, J. A. Zapien, I. Bello, W. J. Zhang, S. T. Lee. Cryst. Grow. & Des. **9**, 7 (2009).
[32] S. M. Zhou, H. C. Gong, B. Zhang, Z. L. Du, X. T. Zhang, S. X. Wu. Nanotechnology **19**, 17 (2008).
[33] X. Shen, G. Wang, D. Wexler. Senso. Actua. B: Chem. **143**, 1 (2009).
[34] Y. Sheng, Y. Jiang, X. Lan, C. Wang, S. Li, X. Liu, H. Zhong. J. Nanomater. 2011, (2011).
[35] L. L. Yang, Q. X. Zhao, M. Willander. J. Allo. Comp. **469**, 1-2 (2009).
[36] K. Yu, Z. Jin, X. Liu, Z. Liu, Y. Fu. Mater. Lett. **61**, 13 (2007).
[37] Y. Tak, K. Yong. J. Phys. Chem. B **109**, 41 (2005).
[38] R. Shi, P. Yang, X. Dong, Q. Ma, A. Zhang. Appl. Surf. Sci. 264, (2013).
[39] A. Dev, S. Kar, S. Chakrabarti, S. Chaudhuri. Nanotechnology **17**, 5 (2006).

*Corresponding author: dlili104@sina.com